Mesospheric energy loss rates by OH and O2 emissions at 23°S

P. R. Fagundes, D. Gobbi, H. Takahashi, Y. Sahai

Ann. Geophysicae 15, 797–804 (1997) © EGS – Springer-Verlag 1997

Annales Geophysicae

Mesospheric energy loss rates by OH and O_2 emissions at 23°S

P. R. Fagundes*, D. Gobbi, H. Takahashi, Y. Sahai

Instituto Nacional de Pesquisas Espaciais-INPE-C.P. 515-12.201-970-São José des Campos, SP, Brazil;
e-mail: fagundes@fislume.laser.impe.br
*Also at: Universidade do Vale do Paraíbs-UNIVAP-IP&D, Urbanova, S. José des Campos, SP, Brazil

Received: 4 July 1995 / Revised: 18 December 1996 / Accepted: 13 January 1997

Abstract. The nightglow OH(9, 4) and O_2 atmospheric (0,1) band emission intensities and their rotational temperatures T(OH) and T(O_2), respectively, observed at Cachoeira Paulista (23°S, 45°W), Brazil, during the period from October 1989 to December 1990, have been analyzed to study the nighttime mesospheric energy loss rates through the radiations from the vibrationally excited OH^* and electronically excited O_2^* bands. The total emission rates of the OH Meinel bands, O_2 atmospheric (0,0) and O_2 infrared atmospheric ($^1\Delta_g$) bands were calculated using reported data for the relative band intensities $I_{(v'',v')}/I_{(9,4)}, I_{O_2A(0,0)}/I_{O_2A(0,1)}$ and $I_{O_2(^1\Delta_g)}/I_{O_2A(0,1)}$. It was found that there is a minimum in equivalent energy loss rate by the OH^* Meinel bands during December/January (equivalent energy loss rate of 0.39 K/day*, where day* means averaged over the night) and maximum in equivalent energy loss rate during September (equivalent energy loss rate of 0.98 K/day*). Energy loss rate by the O_2^* radiation, on the other hand, is weaker than that by the OH^* Meinel bands, showing equivalent energy loss rates of 0.12 K/day* and 0.22 K/day* during January and September, respectively.

1 Introduction

Several investigators have studied the propagation of waves in the mesosphere (tides and gravity waves) using ground-based observations of mesospheric nightglow emissions, e.g., NaD 589.3 nm, OH Meinel bands, O_2 atmospheric (0,1) band and OI 557.7 nm (Krassovsky, 1972; Misawa and Takeuchi, 1977; Takahashi *et al.*, 1985; Taylor *et al.*, 1987; Myrabø and Harang, 1988; Fagundes *et al.*, 1995). However, only a few investigations (e.g., Fukuyama, 1974; Mlynczak and Solomon, 1991, 1993; McDade and Llewellyn, 1991) have been dedicated to study these emissions as a mesospheric energy loss mechanism and how these emissions would affect the mesospheric heat budget, since they reduce the amount of energy available for heat in the mesosphere. Energy loss through optical radiations of the vibrationally excited $OH^*(v', v'')$ and electronically excited O_2^* airglow are important channels of the heat budget in the mesospheric region. The OI 557.7 nm and NaD airglow emissions, on the other hand, may be neglected for the heat budget in this region (Fukuyama, 1974), since the energy associated with these two atomic emissions (OI 557.7 nm and NaD 589.3 nm) are much smaller than those from the molecular band emissions.

During the daytime the solar UV energy is absorbed mainly by O_2 and O_3 (photodissociation and photoionization) in the mesosphere and lower thermosphere. The absorbed UV energy is deposited in multi-step process in three different channels: (a) translational energy, (b) chemical potential energy and (c) atomic and molecular internal energy. The energy which was accumulated in chemical form is released primarily through exothermic chemical reactions leading to chemical heating (translational energy), but if the products formed by the chemical reactions are electronically or vibrationally excited (O^*, OH^* and O_2^*), then a fraction of the chemical energy will be converted into atomic and molecular internal energy and it may be radiated away in the form of photons, reducing the chemical heating, so the O^*, O_2^* and OH^* emissions reduce the heating efficiency of the exothermic chemical reactions. Atmospheric cooling by spontaneous emission may occur when translational energy is converted into molecular internal energy and re-radiated in photons as in the case of CO_2 at 15 μm. Details about the mesosphere and lower thermosphere heating budget have been well reviewed by Mlynczak and Solomon (1993).

According to the first law of thermodynamics the energy change in a system is equal to the net energy transfer across the boundaries of the system. Therefore,

Correspondence to: T. R. Fagundes

to describe the time variation of the temperature in the mesosphere, all kinds of energy, such as chemical potential, kinetic, thermal, radiant, etc., should be included. It should also consider sources and sinks of energy, i.e., vertical and horizontal transports and conduction, and energy transformation to and from kinetic, internal and chemical potential. However, it is possible to calculate each energy channel described in a parametric way. In this work we have calculated and discussed important features of the reduction of chemical heating by airglow radiations in the mesospheric region at 23°S.

2 Observations

Regular zenith observations of the NaD 589.3 nm, OI 557.7 nm, OI 630.0 nm, OH(9, 4) band and O_2 atmospheric (0, 1) band nightglow emissions have been carried out at Cachoeira Paulista (23°S, 45°W), Brazil, using a multi-channel tilting filter-type photometer. The photometer has a field of view of 2° full angle and uses a cooled Hamamatsu R953-02 (GaAs) photomultiplier. It takes about 3 min to complete one sequence of observation with five interference filters (including background) and dark noise checks (see e.g., Takahashi *et al.*, 1985; 1986). The observed OH(9, 4), and O_2 atmospheric (0, 1) bands emission intensities and their rotational temperatures [hereafter T(OH) and T(O_2)], obtained during the period November 1989 to December 1990, were analyzed to study the nighttime mesospheric energy loss rates by the optical radiations from the vibrationally excited OH^* Meinel bands and electronically excited O_2^* bands. Estimated errors in the absolute intensities for the two emissions are approximately ±15%. In order to calculate the radiation energy loss as a function of the height, the OH(8,3) and O_2 atmospheric (0,0) band volume emission profiles observed at equatorial location (Melo, 1994; Takahashi *et al.*, 1995) were used in the calculations. These simultaneous profiles were obtained during an airglow rocket photometer campaign called MULTIFOT and are the only measured vertical profiles in the Brazilian sector. The payload was launched from Alcântara (2.5°S, 44.4°W), Brazil, on a SONDA III rocket at 23:52 hours local time on 31 May 1992 (Fig. 1).

The overall intensities of the OH Meinel bands and O_2^* bands (O_2 atmospheric (0, 1), O_2 atmospheric (0, 0) and O_2 infrared atmospheric ($^1\Delta_g$) hereafter $O_2b(0,1)$, $O_2b(0,0)$ and $O_2(^1\Delta_g)$, respectively, were inferred from the relative band intensities $I_{(v'',v')}/I_{(9,4)}$, $I_{O_2A(0,0)}/I_{O_2A(0,1)}$ and $I_{O_2(^1\Delta_g)}/I_{O_2A(0,1)}$ published previously by Llewellyn *et al.* ,(1978); Coxon and Foster (1982); Harris (1983); Greer *et al.* (1986) and McDade *et al.* (1986; 1987).

Using the neutral densities from the MSIS-86 model (Hedin, 1987), the estimated total OH Meinel and O_2^* band intensities, the observed vertical profiles of the OH(8,3) and $O_2b(0,0)$ bands and monthly averaged variations of the observed OH(9, 4) and $O_2b(0,1)$ bands, we calculated the equivalent energy loss rates

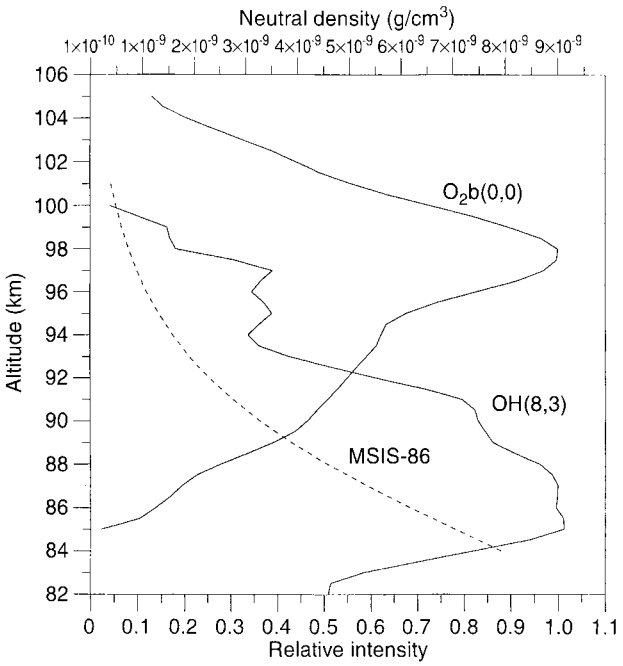

Fig. 1. The OH(8,3) and $O_2b(0,0)$ volume emission profiles obtained from the rocket-borne measurements at Alcântara (2°S, 44°W) (Melo, 1994) and neutral density profile from the MSIS-86 for June at midnight at (23°S, 45°W)

(in K/day*) for the OH Meinel O_2^* bands as a function of altitude.

3 Equivalent energy loss rate by airglow

From thermodynamical principles the reduction in chemical heating in the mesosphere region at a fixed altitude is calculated using the energy loss rate term by airglow emission (OH Meinel and O_2^* bands) according to the following expression,

$$\frac{dT}{dt} = \frac{1}{C_p \rho} Q_{Airglow} \tag{1}$$

where T is the temperature, C_P is the specific heat at constant pressure, ρ is the bulk density of the atmosphere and Q is the energy loss rate by airglow.

The energy loss rate by airglow emission ($Q_{Airglow}$) at a fixed height is given by,

$$Q_{Airglow} = -N_f \frac{hc}{\lambda} \tag{2}$$

where N_f is the number of photons emitted per second per unit volume, $h = 6.63 \times 10^{-34} j\,s$ is Planck's constant, $c = 3 \times 10^8\ \mathrm{m\,s^{-1}}$ is the speed of light and λ is the emission wavelength.

In order to calculate $Q_{Airglow}$ as a function of altitude, we have to transform the observed ground-based intensity, which is measured in Rayleighs (Rayleigh corresponds to 10^6 photons $\mathrm{s^{-1}\ cm^{-2}}$ *per* column) in volume emission rate profile. To obtain this, a weighting function was calculated from the volume emission profile observed by rocket photometer (Melo, 1994), as

$\alpha(z) = I(z)/I_T$ where $I(z)$ is the volume emission rate for 1 km interval in the vertical profile and I_T is the total column volume emission rate of the vertical profile. Notice that $\alpha(z)$ is in step of 1 km and the ground intensity in photons $s^{-1}\,cm^{-2}$/column, so a conversion factor, $\beta = 10$, is necessary to get photons $s^{-1}\,m^{-3}$ units.

Therefore, the energy loss rate for 1 km altitude step is given by,

$$Q_{Airglow}(z) = -10^6\,\alpha(z)\,\beta\frac{I\,hc}{\lambda} \tag{3}$$

where I is the ground-based airglow intensity in Rayleighs.

3.1 Equivalent energy loss rate by the OH Meinel band at 84–93 km altitude

Using the observed nighttime $OH^*(9,4)$ band intensities and the OH Meinel band intensities calculated by Llewellyn *et al.* (1978) for nightglow, a relationship between the observed OH(9, 4) band intensity and other OH^* bands can be obtained (see Table 1). In order to calculate the photon energy of the individual band, we calculated the band origin as a reference wavelength where the rotational band structure of the $OH^*(v', v'')$ located. The wavelengths of the OH^* band origin (see Table 2) were calculated using molecular constants given by Coxon and Foster (1982).

Thus the equivalent energy loss rate term by the OH^* Meinel band is given by

$$\frac{dT}{dt} = -\frac{\alpha_1(z)\beta}{C_p}\,\frac{I_{(9,4)}(t)}{\rho(z,t)}\,10^6\sum_{v''=9}^{1}\sum_{v'<v''}^{0}\frac{I_{(v'',v')}}{I_{(9,4)}}\frac{h\,c}{\lambda_{(v'',v')}} \tag{4}$$

and using Tables 1 and 2 we can calculate the following summation,

$$\sum_{v''=9}^{1}\sum_{v'<v''}^{0}\frac{I_{(v'',v')}}{I_{(9,4)}}\frac{h\,c}{\lambda_{(v'',v')}} = 1.70\times10^{-16}. \tag{5}$$

Using the observed OH(8, 3) emission profile (see Fig. 1) from the rocket measurements obtained at Alcântara, Brazil, (Melo, 1994), we can estimate the fraction of the column emission rates between 84 and 93 km of altitude (see Table 3); where $\alpha_1 = I_h/I_T$ [I_h is the measured vertical profile of the OH(8,3) emission rate at a fixed altitude and I_T is the OH(8, 3) band total column emission rate; see Table 3] and $\beta = 10$. Also, using the neutral gas density from the MSIS-86 model and $C_p = 1012.71\,J/kg\,K$, the equivalent energy loss rate during the night due to the OH airglow can be calculated as a function of altitude from the following equation

$$\frac{dT}{dt} = -1.68\times10^{-12}\alpha_1(z)\frac{I_{(9,4)}(t)}{\rho(z,t)} \tag{6}$$

which in integral form is

$$\Delta T = -1.68\times10^{-12}\alpha_1(z)\int_t\frac{I_{(9,4)}(t)dt}{\rho(z,t)} \tag{7}$$

Finally Eq. (7) is integrated using $I_{OH(9,4)}(t)$ and $\rho(z,t)$ with a time resolution of 5 min.

3.2 Equivalent energy loss rate by the O_2^* at 92–101 km altitude

The equivalent energy loss rate by O_2^* is calculated using the observed nighttime O_2b(0,1) at 864.5 nm band intensity and the relationship between the band intensities IO_2^*/IO_2b(0,1),

Table 1. Calculated relative band intensities $I(v'', v')/I(9, 4)$ using Llewellyn *et al.* (1978)

v''	0	1	2	3	4	5	6	7	8
v'1	139.26702								
2	52.530541	94.58988							
3	2.1815009	94.76440	50.436300						
4	0.1308901	7.137871	120.76789	20.418848					
5	0.0645724	0.507853	13.752182	139.9651	5.794066				
6	0.0052356	0.052356	1.2739965	21.116928	142.2339	2.356021			
7	0.0010471	0.022688	0.1588133	2.513089	32.28621	140.8377	7.888307		
8	0.0003490	0.007504	0.0261780	0.4904014	5.7759162	52.53054	144.3281	22.33857	
9	0.0001169	0.002618	0.0092496	0.1099476	1	9.075044	75.91623	123.5602	42.5829

Table 2. Calculated wavelengths λ (nm) of the OH^* band origin (Coxon and Foster, 1982)

v''	0	1	2	3	4	5	6	7	8
v'1	2801.40								
2	1433.96	2937.69							
3	979.04	1505.03	3086.08						
4	752.34	1028.58	1587.75	3249.10					
5	617.01	791.30	1083.02	1668.59	3430.18				
6	527.46	649.81	834.37	1143.54	1764.60	3634.12			
7	469.16	556.34	686.31	882.59	1211.76	1873.65	3867.75		
8	417.38	490.45	588.74	727.54	937.46	1290.01	1999.93	4141.32	
9	381.38	441.96	520.23	625.70	774.94	1001.11	1381.74	2149.73	4470.14

Table 3. Observed fraction of the column emission rate as a function of altitude for the OH(8, 3) and $O_2A(0,0)$ (Melo, 1994) where $\alpha = I_h/I_T$ (I_h is the observed column emission rate at a fixed altitude and I_T is the observed total column emission rate)

OH(8, 3)		$O_2A(0,0)$	
km	$\alpha_1 = I_h/I_T\%$	Km	$\alpha_2 = I_h/I_T\%$
84	8.48	92	5.33
85	9.18	93	5.73
86	9.10	94	5.98
87	8.97	95	6.98
88	8.27	96	8.50
89	7.70	97	9.30
90	7.47	98	8.98
91	6.43	99	7.65
92	4.72	100	5.98
93	3.35	101	4.62

$$\frac{dT}{dt} = -\frac{\alpha_2(Z)\beta}{C_p}\,\frac{I_{O_2b(0,1)}(t)}{\rho(z,t)}\,10^6 hc \left[\frac{1}{\lambda_{O_2b(0,1)}} + \frac{I_{O_2b(0,0)}}{I_{O_2b(0,1)}\lambda_{O_2b(0,0)}} + \frac{I_{O_2(\Delta)}}{I_{O_2b(0,1)}\lambda_{O_2(\Delta)}}\right] \quad (8)$$

The relationship between the relative band intensities of the $O_2b(0,1)$ at 864.5, $O_2b(0,0)$ at 761.9 and $O_2(^1\Delta_g)$ at 1.27 μm are less studied especially at low latitudes. However, from ETON rocket experiments at high latitudes we have the relationships $O_2b(0,0)/O_2b(0,1) = 17$ and $O_2(^1\Delta_g)/O_2b(0,0) = 20$ (Harris, 1983; Greer *et al.*, 1986; McDade *et al.*, 1986; 1987) and these have been used here. Therefore, a part of the right-hand side of Eq. 8 using the relationship between the intensities (Table 4), can be transformed in:

$$h\,c\left[\frac{1}{864.5\times10^{-9}} + \frac{17}{761.9\times10^{-9}} + \frac{348}{1270\times10^{-9}}\right]. = 1.01\times10^{-17} \quad (9)$$

Also, from the observed $O_2b(0,0)$ emission profile (see Fig. 1) at equatorial latitude (Melo, 1994) we can estimate the fraction of the column emission rates between 92 to 101 km (see Table 3), where $\alpha_2 = I_h/I_T$ [I_h is the measured $O_2b(0,0)$ emission profile at fixed altitude and I_T is the measured vertical $O_2b(0,0)$ total column emission rate], $\beta = 10$, $C_p = 1013.77$ J/kg K and $\rho(z,t)$ is the neutral gas density used from the MSIS-86. Thus, the expression for the equivalent energy loss rate gives,

$$\frac{dT}{dt} = -9.96\times10^{-14}\,\alpha_2(z)\,\frac{I_{O_2b(0,1)}(t)}{\rho(z,t)} \quad (10)$$

Table 4. Relative band intensities IO_2^*/IO_2A (0,1) and wavelengths of the O_2^* band origin

	$O_2A(0,1)$	$O_2A(0,0)$	$O_2(^1\Delta_g)(0,0)$
$O_2A(0,1)$	1	17	348
λ	864.5 nm	761.9 nm	1.27 μm

which in integral form is

$$\Delta T = -9.96\times10^{-14}\,\alpha_2(z)\int_t \frac{I_{O_2b(0,1)}(t)dt}{\rho(z,t)}. \quad (11)$$

Finally Eq. (11) is integrated using $I_{O_2b(0,1)}(t)$ and $\rho(z,t)$ with a time resolution of 5 min.

4 Results and discussion

The monthly averaged OH(9, 4) and $O_2b(0, 1)$ band emission intensities and their rotational temperatures T(OH) and $T(O_2)$ are plotted in Fig. 2. Due to bad weather conditions, there are some months in which we did not get any useful data. In spite of this, the data are sufficient for a seasonal variation study. The seasonal variations of the monthly means of the intensities and rotational temperatures presented in this study agree with some previous works by Takahashi *et al.* (1977; 1984; 1986) from the same location.

The monthly averaged nocturnal variations of the observed OH(9,4) and $O_2b(0,1)$ band emission intensities were used to study the seasonal equivalent energy loss rates by these emissions at Cachoeira Paulista (23°S). In Fig. 3 we show the monthly averaged nocturnal variations of the OH(9, 4), $O_2b(0,1)$, T(OH) and $T(O_2)$ for June as an example. Also, in Fig. 3, the monthly averaged nocturnal rotational temperature variations (T(OH) and $T(O_2)$) show oscillations of

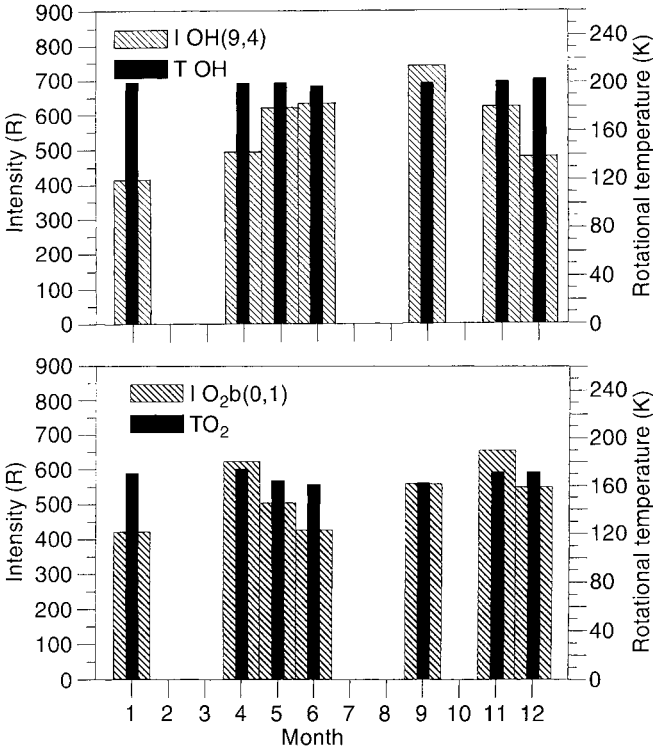

Fig. 2. Monthly means of the OH(9,4) and $O_2b(0,0)$ intensities and T(OH) and $T(O_2)$ rotational temperatures observed at Cachoeira Paulista (23°S, 45°W)

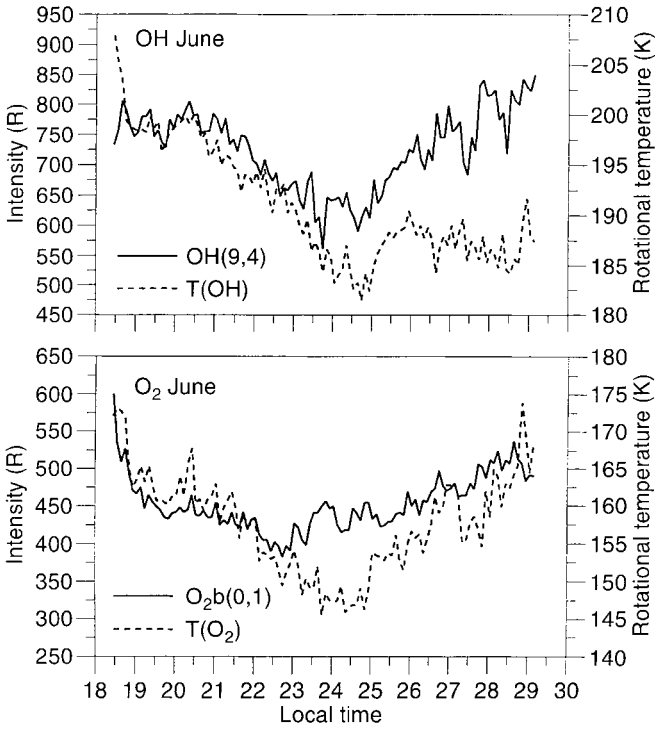

Fig. 3. Average nocturnal variations of the OH(9, 4) and $O_2b(0, 0)$ intensities used to calculate the energy loss rates and the rotational temperatures T(OH) and $T(O_2)$ for June

about 30 K during the course of night. These oscillations of the rotational temperatures are produced most probably by tides and/or gravity waves and the energy dissipated by these waves also plays a significant role in the mesospheric heat budget. However, the present observations do not allow us to estimate the energy dissipated by these waves and further investigations of the vertical and horizontal wave parameters are necessary for a more detailed study.

In order to calculate the monthly averaged nocturnal equivalent energy loss rates (in K/day*) by the OH^* and O_2^* bands at a fixed height, the time integrations in Eqs. (7) and (11) were carried out with a time resolution of 5 min. where $I_{OH(9,4)}(t)$ and $I_{O_2(0,1)}(t)$ are the monthly averaged nocturnal variations of the OH(9,4) and $O_2b(0, 1)$ emission intensities (see e.g., in Fig. 3), $\alpha_1(z)$ and $\alpha_2(z)$ are used from Table 3 and $\rho(z, t)$ was taken from the MSIS-86 model for the appropriate local time and altitude.

In Fig. 4 we show the results for seven months of the total nocturnal equivalent energy loss rates as a function of altitude for OH^* and O_2^* bands, in K/day* (where day* means averaged over the night of about 10 hours of observations). It may be noted that the equivalent energy loss rates by the OH^* and O_2^* emission show a very clear seasonal variation and also the equivalent energy loss rates by the OH^* emission are stronger than those by the O_2^* emission. The calculations for the OH^* energy loss showed a maximum energy loss of about 0.98 K/day* during September and a minimum of 0.39 K/day* during December/January and for O_2^* a maximum of 0.26 K/day* during April and a minimum of 0.1 K/day* during December/January. Therefore, during some months the OH^* Meinel band may be an important contributor to the mesospheric heat budget.

In addition, it is observed from Figs. 1 and 4 that the peak equivalent energy loss rates are about 4 km and 2 km above the OH^* and O_2^* peak emission profiles, respectively. This behavior of the equivalent energy loss rate profiles is consistent, since the neutral density decays much faster (exponentially) with altitude compared with the upper part of the emission layer used in this work. Therefore, the peak equivalent energy loss rates will be higher than the peak emission profiles if the upper part of the OH^* and O_2^* emission layer decays slower than an exponential rate.

The shape and peak heights of the emission layer's change during the course of night are most probably produced by waves and chemical processes. Furthermore, there is no information available related to seasonal changes in the shape and peak heights of the OH^* and O_2^* emissions in the region where this study was carried out. To investigate the dependence of the energy loss rates on the peak height variations, the neutral atmosphere was fixed and the observed profiles were moved 1 km up and down and the energy loss rates were calculated for these two extreme cases. In Fig. 5 we show the behavior of the energy loss rates for the months which presented the maximum and minimum energy loss rates. Therefore, when the emission profiles were shifted up and down by 1 km we notice that the energy loss rate presented a small change in the bottom side profile, however, in the upper side profile change of about 20% was observed.

Since the investigations presented assumes same peak heights and shapes of the emission layers for all the months studied and extension of the observed equatorial profiles to low latitude regions, it is very important to compare the present results with those published earlier. These comparisons have been made with Fukuyama (1974) and Mlynczak and Solomon (1993).

Using a photochemical model Fukuyama (1974) investigated the equivalent energy loss rate (which was called cooling) by airglow emissions and showed a maximum of the equivalent energy loss rate of about 5–6 K/day near 85 km by the OH Meinel band and 0.5 and 2 K/day in the region 85–90 km by the O_2 atmospheric and $O_2(^1\Delta_g)$ infrared atmospheric bands, respectively.

Our present study shows that the monthly equivalent energy loss rate variations by the OH Meinel bands is 0.12 to 0.98 K/day* and therefore are smaller than those reported by Fukuyama (1974), 5 to 6 K/day. Note that Fukuyama's (1974) calculations were carried out for a full day (24 h), whereas the present calculations were carried out only for the nighttime (about 10 h), but the estimated energy loss during the night at Cachoeira Paulista should be 3 or 4 times larger to agree with Fukuyama's (1974) photochemical model, since the dayglow due to the OH Meinel system intensity is about 1/3 of the nightglow OH Meinel band (Llewellyn *et al.*, 1978). Furthermore, the present study shows that the equivalent energy loss rate peaks due to the OH Meinel

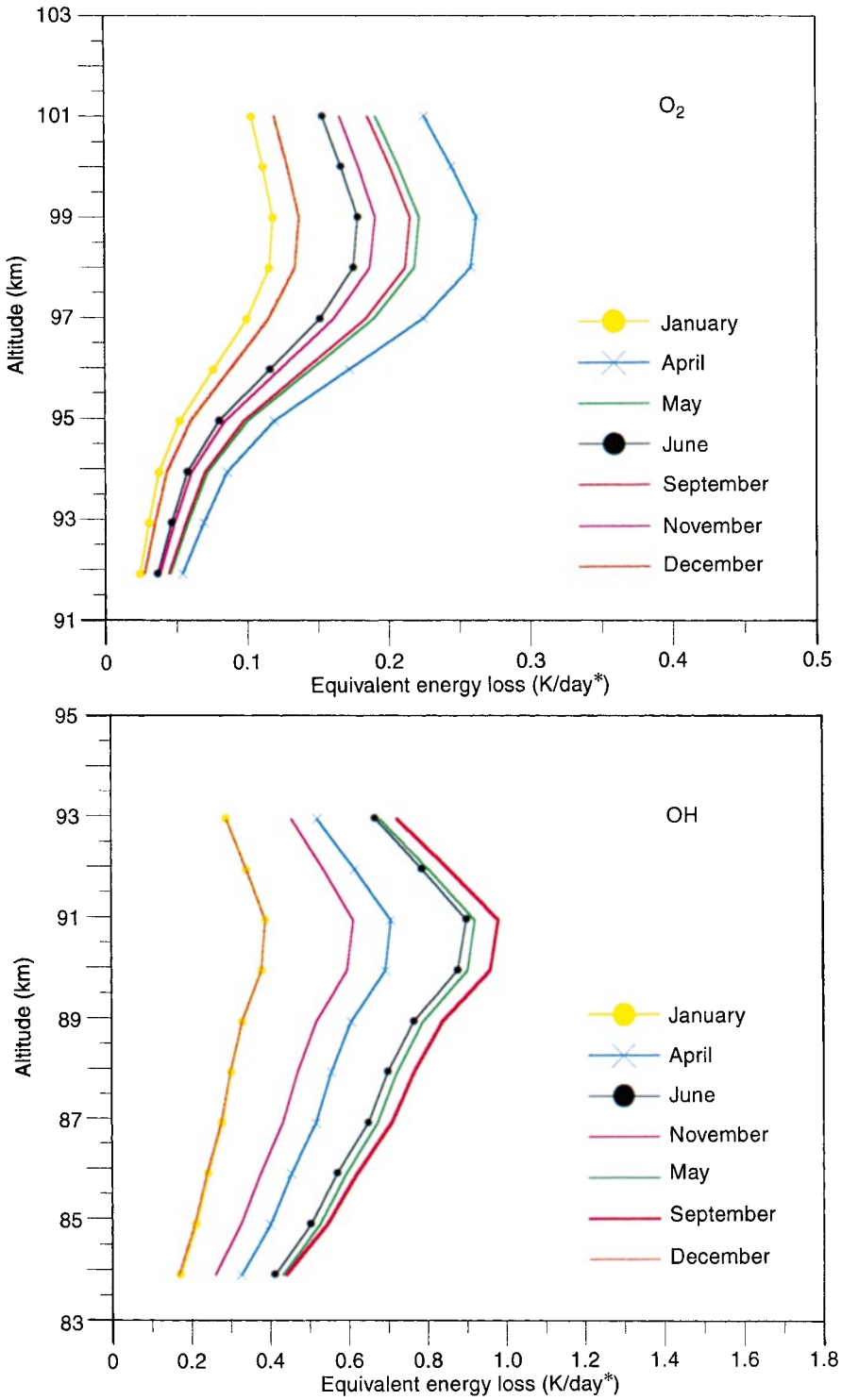

Fig. 4. Monthly equivalent energy loss rates (in K/day*) due to the OH Meinel and O_2^* band airglow emissions as a function of altitude

and O_2^* bands are higher than those presented by Fukuyama (1974). Possible sources for discrepancies detected between our calculations and Fukuyama photochemical model may be the reaction rate constants and minor constituents concentrations. Since then, the reaction rate constants and the minor constituents concentrations have been improved and updated during the last decade.

However, Mlynczak and Solomon (1993) using the recent reaction rate constants and minor constituents showed that the energy loss rate by OH^* emissions is 0.6 K/day and it is less than 10% of the total available chemical heating rate for the $H + O_3$ reaction which leads to OH^*. The energy loss rate by O_2^* emission (excluding O_2 infrared atmospheric band) is 0.1 K/day and the heating associated with O-atom recombination reached a maximum of 7 K/day. Mlynczak and Solomon's (1993) energy loss rate results by OH Meinel bands and O_2^* emission are compable with those reported in this study.

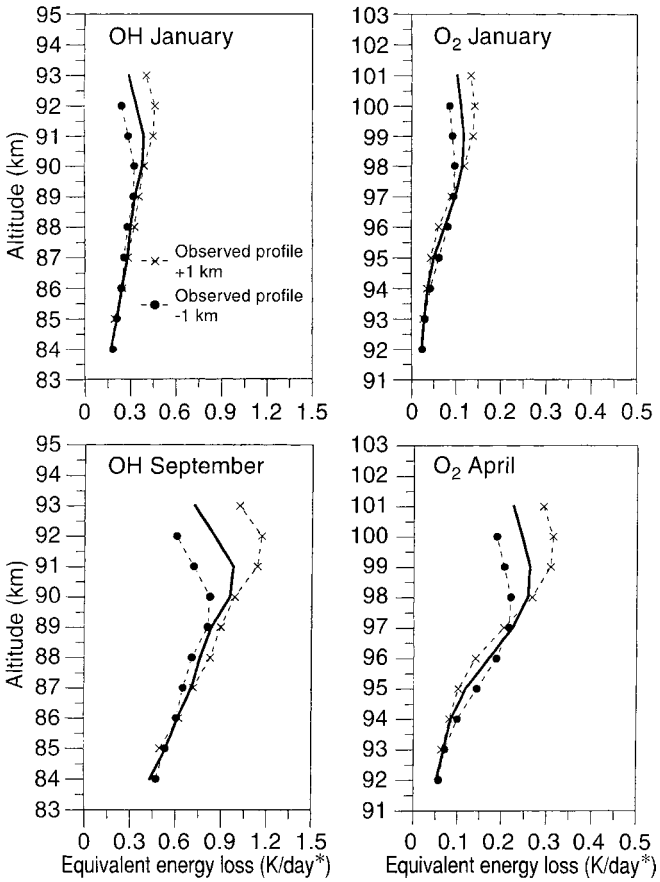

Fig. 5. Equivalent energy loss rates (in K/day*) due to the OH Meinel and O_2^* bands as a function of altitude for the observed profile and when this observed profile is shifted up and down by 1 km

4.1 Uncertainties in the parameters used to determine the energy loss rates

An important feature presented in this work is that there is a strong seasonal variation in the equivalent energy loss rates from the OH Meinel and O_2^* bands (more than 130%) and that the peaks in the energy loss rates by these emissions are higher than the airglow peak profiles. However, there are several uncertainties such as ±15% in the observed OH(9,4) and $O_2b(0,1)$ band intensities, transition probabilities and background atmosphere model (MSIS-86). This work has also some limitation as the vertical emission rate profiles used was taken at 20° latitude away from the ground based observations and these profiles were used for all the months.

It is well known that there are temporal and seasonal variations in the vertical emission profiles, emission intensities and background atmosphere associated with atmospheric motions (tides and gravity waves) and this can lead to day-today variability of the parameters used in our calculations. Takahashi *et al.* (1986) showed that mesospheric emissions ($O_2b(0,1)$ and OH(9, 4)) intensities presented daily variations reaching about 25% of the standard deviation of the montly mean values. Therefore, the atmospheric motions influence the daily variations in the energy loss rates by airglow. However, the main purpose of our analysis is to show the mesospheric monthly variability of the equivalent energy loss rate by airglow.

The error of ±15% in the observed OH(9, 4) and $O_2b(0,1)$ emission intensities will result in similar error in the total emission rates of the OH Meinel and O_2^* bands, since the energy loss rate by the airglow calculated is linearly proportional to the observed emission intensities, the error will be also of the order of ±15%.

The OH^* relative band intensities used in this study was taken from Llewellyn *et al.* (1978) which was based on Mies' (1974) radiative lifetimes of the OH Meinel bands. However, according to Mlynczak and Solomon (1993) there is no significant difference between the heating rates calculated using Mies' (1974) and Turnbull and Lowe's (1989) Einstein coefficients. Mlynczak and Solomon (1993) also pointed out that there is a significant difference (40%) when they used more recent unpublished coefficients. In addition, there are some doubts regarding the relative band intensities and at present these are still subject to discussion (for more details see Johnston and Broadfoot, 1993). The peak heights in the emission rate profiles and shapes of the different OH^* bands (e.g. OH(8, 3) and OH(9, 4)) present small differences (Lopez-Moreno *et al.*, 1987).

We must point out that there are more uncertainties in the calculations for the O_2^* energy loss rate, since the relative band intensities rates $I_{O_2A(0,0)}/I_{O_2A(0,1)}$, $I_{O_2(^1\Delta_g)}/I_{O_2A(0,1)}$, and the emission profile and shape of the $O_2(^1\Delta_g)$ are not well studied at low latitudes. Also, our calculations showed that the maximum energy loss rate by O_2^* is only about 0.12 to 0.26 K/day* during some months and it may be less significant in the mesospheric heat budget.

In order to study how the equivalent energy loss rate changes when the emission rate profiles (OH^* and O_2^*) move upward or downward, a simulation was carried out shifting the emission rate profiles by 1 km upward and downward, and keeping background atmosphere fixed. These simulations showed that when the emission profiles were displaced by only 1 km, there are changes in the peak equivalent energy loss rates by about 20% (see Fig. 5), increasing when the layer moves up and decreasing when the layer goes down.

5 Conclusions

Using the monthly averaged nocturnal variations of the OH(9, 4) and $O_2b(0,1)$ band emission intensities measured at Cachoeira Paulista (23°S, 45°W), the observed volume emission profiles OH(8, 3) and $O_2b(0,0)$ at Alcântara (2°S, 44°W) and the MSIS-86 model for the neutral density, the mesospheric equivalent energy loss rates by the OH^* Meinel and O_2^* [atmospheric (0, 1), (0, 0) and infrared atmospheric $(^1\Delta_g)$] bands were calculated for several months. The main results are as follows:

a. The equivalent energy loss rate by the OH^* Meinel emission bands shows a seasonal variation with a minimum during December/January (0.39 K/day*) and a maximum during September (0.98 K/day*).
b. The equivalent energy loss rate by the O_2^* emission bands shows a seasonal variation with a minimum during December/January (0.1 k/day*) and a maximum during April (0.26 K/day*).
c. The equivalent energy loss rate by the OH^* bands is stronger than that by the O_2^* bands, by about 4 to 5 times.
d. The equivalent energy loss rates of the OH^* and O_2^* bands showed a maximum at heights of 91 and 99 km, respectively. These maximum heights in the equivalent energy loss rates are about 4 km and 2 km above the respective airglow emission peaks OH^* and O_2^*.
e. For both the OH^* and O_2^* bands the peaks in the equivalent energy loss rates are larger (about 20%) when the emissions profiles are shifted upward and smaller (about 20%) when the profiles are shifted downward.

Acknowledgements. Thanks are due to Dr. S.M.L. Melo for providing the equatorial OH(8, 3) and $O_2b(0,0)$ airglow profiles. Partial funding for this work was provided through the Conselho Nacional de Desenvolvimento Cientifico e Tecnologico, process CNPq 300955/93-6.

Topical Editor F. Vial thanks W. Ward for his help in evaluating this paper.

References

Coxon, J. A., and S. C. Foster, Rotational analyses of hydroxyl vibrational-rotational emission bands: molecular constants for OH $X^2\Pi$, $6 \leq v \leq 10$, *Can. J. Phys.*, **60,** 41, 1982.

Fagundes, P. R., H. Takahashi, Y. Sahai, and D. Gobbi, Observation of gravity waves from multispectral mesospheric nightglow emission observed at 23°S, *J. Atmos. Terr. Phys.*, **57,** 395, 1995.

Fukuyama, K., Latitudinal distributions of photochemical heating rates in the winter mesosphere and lower thermosphere, *J. Atmos. Terr. Phys.*, **36,** 1321, 1974.

Greer, R. G. H., D. P. Murtagh, I. C. McDade. P. H. G. Dikinson, L. Thomas, D. B. Jenkins, J. Stegman, E. J. Llewellyn, G. Witt, D. J. Mackinnon, and E. R. Williams, ETON1: a data base experiment to study of energy transfer in the oxygen nightglow, *Planet. Space Sci.*, **34,** 771, 1986.

Harris, F. R., The atmospheric system of O_2 in nightglow, *EOS,* **64,** 779, 1983.

Hedin, A. E., MSIS-86 thermospheric model, *J. Geophys. Res.*, **88,** 170, 1987.

Johnston, J. E., and A. L. Broadfoot, Midlatitude observations of the night airglow: implications to quenching near the mesopause, *J. Geophys. Res.*, **98,** 21, 603, 1993.

Krassovsky V. I., Infrasonic variations of OH emission in the upper atmosphere. *Ann. Geophysicae*, **28**, 739, 1972.

Llewellyn, E. J., B. H. Long, and B. H. Solheim, The quenching of OH^* in the atmosphere, *Planet. Space Sci.*, **26,** 525, 1978.

Lopez-Moreno, J. J., R. Rodrigo, F. Moreno, M. Lopez-Puertas, and A. Molina, Altitude distribution of vibrationally excited states of atmospheric hydroxyl at levels $v = 2$ to 7, *Planet. Space Sci.*, **35,** 1029, 1987.

Melo, S. M. L., Aeroluminescência da região equatorial: Estudo via experimento de foquete Ph.D. Thesis, INPE-5589-TDI/551, 1994.

McDade, I. C., and E. J. Llewellyn, Comment on "Middle atmosphere heating exothermic chemical reactions involving odd-hydrogen species", *Geophys. Res. Lett.*, **18**(9), 1791–1792, 1991.

McDade, I. C., D. P. Murtagh, R. G. H. Greer, P. H. G. Dickinson, E. J. Llewellyn, L. Thomas, and D. B. Jenkins, Eton 2: quenching parameters for the proposed precursors of $O_2(b^1\Sigma_g)$ and $O(^1S)$ in the terrestrial nightglow, *Planet. Space Sci.*, **9,** 785, 1986.

McDade, J. C., E. J. Llewellyn, R. G. H. Greer, and D. P. Murtagh, Eton 6: a rocket measurement of the O_2 infrared atmospheric (0,0) band in the nightglow, *Planet. Space Sci*, **15,** 1541, 1987.

Mies, F. H., Calculated vibrational transition probabilities of $OH(X^2\Pi)$, *J. Mol. Spectrosc.*, **54,** 150–188, 1974.

Misawa K., and I. Takeuchi, Ground observation of the $O_2(0,1)$ atmospheric band at 8645 Å and [OI] 5577-Å line, *J. Geophys. Res.*, **82,** 2410, 1977.

Mlynczak, M. G. and S. Solomon, Middle atmosphere heating by exothermic chemical reactions involving odd-hydrogen species, *Geophys. Res. Lett.*, **18**(1), 37–40, 1991.

Mlynczak, M. G., and S. Solomon, A detailed evaluation of the heating efficiency in the middle atmosphere, *J. Geophys. Res.* **98**(6), 10517–10541, 1993.

Myrabø, H. K., and O. E. Harang, Temperatures and tides in the high latitude mesopause region as observed in the OH night airglow emissions, *J. Atmos. Terr. Phys.*, **50,** 739, 1988.

Takahashi, H., Y. Sahai, R. B. Clemesha, P. P. Batista, and N. R. Teixeira, Diurnal and seasonal variations of the OH(8,3) airglow band and its correlation with OI 5577 Å, *Planet. Space Sci.*, **25,** 541, 1977.

Takahashi, H., Y. Sahai, and P. P. Batista, Tidal and solar cycle effects on the OI 5577 Å, NaD and OH(8,3) airglow emissions observed at 23°S, *Planet. Space Sci.*,**32,** 897, 1984.

Takahashi, H., P. P. Batista, Y. Sahai, and R. B. Clemesha, Atmospheric wave propagations in the mesopause region observed by the OH(8,3) band, NaD, O_2 (8645 Å) band OI 5577 Å nightglow emissions, *Planet. Space Sci.*, **33,** 381, 1985.

Takahashi, H., Y. Sahai, and P. P. Batista, Airglow $O_2(^1\Sigma)$ atmospheric band at 8645 Å and the rotational temperature observed at 23°S, *Planet. Space Sci.*, **34,** 301, 1986.

Taylor M. J., M. A. Hapgood, and P. Rothwell, Observations of gravity wave propagation in the OI (OI 557.7 nm, Na (589.2) and near infrared OH nightglow emissions, *Planet. Space Sci.*, **35,** 413, 1987.

Turnbull, D. N., and R. P. Lowe, New hydroxyl transition probabilities and their importance in airglow studies, *Planet Space Sci.*, **33,** 723–738, 1989.